miR-30c reduces myocardial ischemia/reperfusion injury by targeting SOX9 and suppressing pyroptosis

JIA NIE[1*], WENJING ZHOU[1,2*], SHOUYANG YU[2], SONG CAO[1,2], HAIYING WANG[1,2] and TIAN YU[2]

[1]Department of Anesthesiology, Affiliated Hospital of Zunyi Medical University; [2]Guizhou Key Laboratory of Anesthesia and Organ Protection, Zunyi Medical University, Zunyi, Guizhou 563000, P.R. China

Received November 9, 2022; Accepted February 10, 2023

DOI: 10.3892/etm.2023.11879

Abstract. MicroRNAs (miRNAs or miRs) are commonly involved in regulating myocardial ischemia/reperfusion (I/R) injury by binding and silencing their target genes. However, whether miRNAs regulate myocardial I/R-induced pyroptosis remains unclear. The present study established an *in vivo* rat model of myocardial I/R injury and *in vitro* hypoxia/reoxygenation (H/R) injury model in rat primary cardiomyocytes to investigate the function and the underlying mechanisms of miRNAs on I/R injury-induced pyroptosis. RNA sequencing was utilized to select the candidate miRNAs between normal and I/R group. Reverse transcription-quantitative PCR and western blotting were performed to detect candidate miRNAs (miR-30c-5p, also known as miR-30c) and SRY-related high mobility group-box gene 9 (SOX9) expression, as well as expression of pyroptosis-associated proteins (NF-κB, ASC, caspase-1, NLRP3) in the myocardial I/R model. ELISA was used to measure pyroptosis-associated inflammatory markers IL-18 and IL-1β. Moreover, the link between miR-30c and SOX9 was predicted using bioinformatics and luciferase reporter assay. In myocardial I/R injured rats, miR-30c was downregulated, while the expression of SOX9 was upregulated. Overexpression of miR-30c inhibited pyroptosis both *in vivo* and *in vitro*. Furthermore, miR-30c negatively regulated SOX9 expression by binding its 3'untranslated region. In conclusion, the miR-30c/SOX9 axis decreased myocardial I/R injury by suppressing pyroptosis, which may be a potential therapeutic target.

Correspondence to: Dr Haiying Wang, Department of Anesthesiology, Affiliated Hospital of Zunyi Medical University, 149 Dalian Street, Zunyi, Guizhou 563000, P.R. China
E-mail: wanghaiting-8901@163.com

Dr Tian Yu, Guizhou Key Laboratory of Anesthesia and Organ Protection, Zunyi Medical University, 6 West Xuefu Street, Zunyi, Guizhou 563000, P.R. China
E-mail: dllyutian@163.com

*Contributed equally

Key words: microRNA-30c, myocardial ischemia/reperfusion injury, SRY-related high mobility group-Box gene 9, pyroptosis

Introduction

Myocardial ischemia is a pathological condition characterized by interruption of blood supply to myocardium. Reperfusion has become a standard therapy but may lead to irreversible damage to heart tissue, known as myocardial ischemia/reperfusion (MI/R) injury (1), which is a leading cause of mortality worldwide (2). MI/R injury contributes to a range of cardiovascular outcomes, including systolic myocardial dysfunction, cardiac electrophysiology disorder and myocardial death (3,4). Therefore, it is key to determine the underlying mechanisms and develop novel agents to protect myocardial cells during MI/R injury.

Previous studies have identified that microRNAs (miRNAs or miRs) play essential roles in MI/R injury (5-7). miRNAs are small non-coding RNAs 19-22 nucleotides in length. They regulate target mRNAs by binding the sequences in the 3'untranslated regions (3'-UTRs) to facilitate degradation or suppress translation (8). MI/R injury is aggravated by dysregulation of miRNAs. Hinkel *et al* (9) reported that miR-92a is significantly upregulated in pigs subjected to percutaneous I/R. With the utilization of locked nucleic acid-modified antisense miR-92a treatment, infarct size was significantly decreased (9). Similarly, miR-15 family, including miR-15a, miR-15b, miR-16-1, miR-16-2, miR-195 and miR-497, is upregulated in the infarcted region of the heart in response to I/R injury in mice and pigs (10). On the other hand, miRNAs serve as an antagonist in cardiovascular disease. For example, miR-103/107 repairs I/R injury by antagonizing receptor-interacting serine/threonine-protein kinase 1 and 3-dependent necrosis and binding to Fas-associated protein with death domain (11). Overexpression of miR-494 activates the Akt/mitochondrial signaling pathway, resulting in cardioprotective effects against I/R-induced injury in a mouse model (12). Despite many studies (13-15) demonstrating that MI/R injury is associated with microRNAs, the mechanisms are unknown because of the complexity of cellular events. Therefore, it is key to understand the role of miRNAs in MI/R injury.

SRY-related high mobility group-Box gene 9 (SOX9) is a transcription factor of the SRY family, which is involved in cell processes, including oxidation and tumor growth (16-18).

SOX9 is expressed in multiple types of tissue, including lung, brain, and cardiomyocytes (19). SOX9 involved in hepatic (20) and cerebral (21) I/R injury. Suppressing SOX9 markedly decreases hepatic I/R and concurrent injury by inhibiting TGF-β1 activation (20). Moreover, SOX9 plays a vital role in myocardial disease. For example, the loss or inactivation of SOX9 may reduce the initiation of cardiac hypertrophy, fibrosis and inflammation. SOX9 may act as a regulator of myocardial infarction and is involved in crosstalk between myocytes and fibroblasts (22, 23). For example, in patients with ischemic heart disease, the loss of SOX9 may delay the cardiac fibrotic response (24). SOX9 exacerbates hypoxia-induced cardiomyocyte apoptosis by promoting miR-223-3p expression (19). SOX9 suppression by miR-30e elevation protects cardiac function and decreases ventricular remodeling (25). The aforementioned data indicate that SOX9 may be involved in the onset of MI/R injury. However, the underlying molecular mechanism remains unknown. Therefore, the present study aimed to determine the role of miRNAs in regulating MI/R injury and the underlying mechanisms.

Materials and methods

Animal model. Animal experiments were approved [approval no. KLLY(A)-2019-008] and performed in accordance with animal welfare regulations (26) of Zunyi Medical University Committee (Zunyi, Guizhou, China). All experimental procedures were fully compliant with the guidelines for animal research from the National Institutes of Health (27). A total of 84 adult male Sprague-Dawley rats (age, 3 months; weight, ~200 g) that were purchased from Laboratory Animal Center of Third Military Medical University (Chongqing, China) were used in the present study. Animals were housed at 18-22˚C, relative humidity of 50-70% and a 12/12-h light/dark cycle. Food and water were available *ad libitum*. At the end of experiments, all animals were euthanized by intraperitoneal injection of pentobarbital (150 mg/kg).

To establish the MI/R model, rats were divided into I/R or Sham group, n=15 in each group, or I/R + control (n=5), I/R + miR-30c mimics (n=5), I/R + miR-30c inhibitor (n=5). Rats were anesthetized with 45 mg/kg sodium pentobarbital. The rats undergone endotracheal intubation and ventilation (tidal volume, 7 ml; ratio of exhalation/inhalation time, 1.25; breathing rate, 80/min). The thorax was opened by left thoracotomy to expose the heart. A 6.0 prolene suture was used to induce myocardial ischemia by ligating the proximal left anterior descending coronary artery (LAD) with a slipknot. The slipknot was removed after 30 min to allow reperfusion for 30 min. The sham group underwent the same procedure but was not subjected to ligation. Heart samples were obtained for biological and molecular analyses.

Hematoxylin and eosin (H&E) staining. Myocardial tissue samples were collected, fixed with 4% polyformaldehyde at room temperature overnight, dehydrated and then embedded in paraffin. Then the tissues were cut into 5-μm sections. The sections were stained using H&E staining kit (C0105S, Beyotime Institute of Biotechnology) according to the manufacturer's instructions. Images of stained sections were obtained by light microscope at 400x (Nikon Corporation 80i).

ELISA. Serum samples of rats after I/R injury or sham surgery, or cell culture supernatant of isolated RPM cells was collected and centrifugated at 200 x g for 5 min at 4˚C. The serum levels of lactate dehydrogenase (LDH; cat. no. A020-2-2), cardiac troponin I (cTnI; cat. no. H149-2) and creatine kinase isoenzymes (CK; cat. no. A032-1-1) were detected using ELISA kits (all Nanjing Jiancheng Bioengineering Institute) according to the manufacturer's instructions. Levels of IL-18 (cat. no. H015) and IL-1β (cat. no. H002-1-1) in cell culture supernatant and serum samples were determined with commercial kits (both Nanjing Jiancheng Bioengineering Institute) according to the manufacturer's instructions.

Cell culture. 293T cells have high transfection efficiency and are easy to obtain and culture *in vitro* (28). 293T cells were obtained from Nanjing Synthgene Medical Technology, Co., Ltd. Cells were cultured using DMEM (HyClone; Cytiva) supplemented with 10% FBS (Gibco; Thermo Fisher Scientific, Inc.), 1 mM sodium pyruvate and 1% antibiotic-antimycotic (15240-112, Invitrogen, Gibco) at 37˚C in a humidified incubator (Thermo Fisher Scientific, Inc.) with 95% atmosphere and 5% CO_2.

Isolation of rat primary myocardial (RPM) cells and hypoxia/reoxygenation (H/R) treatment. The ventricular tissue of 39 rats heart was excised immediately at the end of reperfusion and cut into small pieces, followed by 5 min digestion with 0.25% pancreatin at 37˚C three times. After centrifugation at room temperature at 1,000 x g for 5 min, RPM cells were collected and cultured according as previously described (29,30). To simulate MI/R injury, FBS/glucose-free DMEM was used and cells were cultured at 37˚C in hypoxic condition (5% CO_2, 94% N_2 and 1% O_2) for 4 h. Then, cells were maintained in normoxic conditions at 37˚C (5% CO_2 and 95% air) for 2 h, as previously described (31). Cells under normoxic conditions at 37˚C for 2 h served as the control group.

Western blotting. RPM cells or myocardium tissue were lysed in RIPA lysis buffer (Beyotime Institute of Biotechnology) supplemented with 1% PMSF (cat. no. 329-98-6, Roche Applied Science) and 1% phosphatase inhibitor (Thermo Fisher Scientific, Inc.). The bicinchoninic acid protein assay kit was used to determine the total protein concentration. Equal amounts of protein (20 mg) from each sample were resolved on 10% SDS-PAGE (Bio-Rad Laboratories, Inc.) and transferred onto polyvinylidene fluoride membrane (Bio-Rad Laboratories, Inc.). Following blocking with 5% milk for 2 h at room temperature, the membranes were incubated with primary antibodies against SOX9 (cat. no. ab185966; 1:1,000), NF-κB p65 (cat. no. ab239882; 1:1,000), NLRP3 (cat. no. ab263899; 1:2,000), apoptosis-associated speck-like protein containing a caspase recruitment domain (ASC; cat. no. ab180799; 1:5,000), caspase-1 (cat. no. ab179515; 1:1,000) and GAPDH (cat. no. ab181602; 1:10,000) overnight at 4˚C. PVDF membranes were incubated at room temperature with horseradish peroxidase-conjugated secondary antibody (goat anti-rabbit IgG H&L; cat. no. ab6721; 1:10,000) for 1 h, then Amersham ECL Western Blotting Detection Reagent (Cytiva, Amersham). The antibodies were all from Abcam. The blots were scanned with a ChemiDoc MP system (Bio-Rad

Laboratories, Inc.). The density of each specific band was measured using ImageJ software V1.52a (National Institutes of Health).

miRNA sequencing. The total RNA was extracted from the heart of MI/R model and sham group rats with TRIzol reagent (Invitrogen, USA). After construction of small RNA libraries using the NEB Next Multiplex Small RNA Library Prep Set for Illumina (catalog # E7330L, New England Biolabs, Inc.), index codes were added to attribute sequences for each sample. Agilent 2100 Bioanalyzer and DNA 1000 chip kit (Agilent, part # 5067-1504) were used to determine the quality of the sequencing library. The length of the library is ~135-155 bp. After PCR products were purified, 140-160 bp DNA fragments were recovered. The concentration of the desired products was determined from the Qubit Fluorometer (Thermo Fisher Scientific, Inc.) and used to prepare an equimolar pool of 7 pM solution for cluster generation on an Illumina flow cell. Finally, single-end reads were sequenced using NovaSeq 6000 SP reagent kit (100 cycles; cat. no. 2002746; Illumina Inc.) with Illumina MiSeq (Illumina, Inc.), as previously described (32). miRDeep2 software (github.com/rajewsky-lab/mirdeep2) was used to predict the novel miRNAs. Then, the trimmed reads were aligned to merged pre-miRNA databases (known pre-miRNA from miRBase v21 plus the newly predicted pre-miRNAs) using Novoalign software (v2.07.11) with at most one mismatch.

Analysis of differentially expressed miRNAs. The expression of miRNAs was determined by the number of reads per million clean tags. Differentially expressed miRNAs were analyzed using DEGseq software v.3.16 (bioconductor.org/packages/release/bioc/html/DESeq.html). For data analysis, differentially expressed miRNA profiles between sham group and I/R group were compared with unpaired t-test. The miRNAs with fold-change >1.5 and P-value <0.05 (33) were defined as differentially expressed miRNAs. Then, hierarchical clustering was performed. miRNAs were selected to verify expression by reverse transcription-quantitative (RT-q) PCR.

RT-qPCR. Total RNA was extracted from RPM cells or heart tissue using TRIzol (Invitrogen, USA) according to the manufacturer's instructions for the analysis of miRNA expression. cDNA was synthesized using a TaqMan™ Advanced miRNA cDNA Synthesis kit (Thermo Fisher Scientific, Inc.) following the manufacturer's protocol. RT-qPCR was performed using TaqMan™ Fast Advanced Master Mix (Thermo Fisher Scientific, Inc.). The thermocycling conditions were as follows: Initial denaturation for 10 min at 95˚C, followed by 40 cycles of 2 sec (95˚C), 20 sec (60˚C) and 10 sec (70˚C), as previously described (34). Quantitative measurements were determined via the $2^{-\Delta\Delta Cq}$ method (31). β-actin and U6 snRNA were used as internal controls for RNA and miRNA, respectively. The primers were designed with the miRNA Design V1.01 (Vazyme Biotech Co., Ltd.) with a universal reverse primer sequence. Primer sequences were as follows: miR-328a-3p: Forward (F), 5'-GCTGGCCCTCTCTGCCC-3' and reverse (R), 5'-AGTGCAGGGTCCGAGGTATT-3'; miR-128-3p: F, 5'-CGCGTCACAGTGAACCGGT-3' and R, 5'-AGTGCAGGGTCCGAGGTATT-3'; miR-148a-3p: F, 5'-GCGCGTCAGTGCACTACAGA-3' and R, 5'-AGTGCAGGGTCCGAGGTATT-3'; miR-676: F, 5'-CGCCGTCCTGAGCTTGTC-3' and R, 5'-AGTGCAGGGTCCGAGGTATT-3'; miR-30d-5p, F: 5'-TGTAAACATCCCCGACTGGA-3' and R, 5'-GAACATGTCTGCGTATCTC-3'; miR-30c-5p: F, 5'-GCGCGTGTAAACATCCTACACT-3' and R, 5'-AGTGCAGGGTCCGAGGTATT-3'; SOX9, F: 5'-GTCGGTGAAGAATGGGCAAG-3' and R, 5'-GACCCTGAGATTGCCCGGA-3'; β-actin: F, 5'-CGCGAGTACAACCTTCTTGC-3' and R, 5'-CGTCATCCATGGCGAACTGG-3' and U6: F, 5'-CTCGCTTCGGCAGCACATATACT-3' and R, 5'-ACGCTTCACGAATTTGCGTGTC-3'.

Luciferase assay. For reporter assay, pMIR-SOX9-3'-UTR-wild-type (WT) and pMIR-SOX9-3'-UTR-mutant (MUT) luciferase reporter plasmids (Nanjing Synthgene Medical Technology, Co., Ltd.) were transfected into 293T cells using Lipofectamine 2000 (Invitrogen; Thermo Fisher Scientific, Inc.). The transfected cells were treated with miR-30c mimics (3'-UCACAUCCUACAAAUGU-5', 100 pmol) or miR-NC (sequence: 5'-CUAACGCAUGCACAGUCGUACG-3'), both from Nanjing Synthgene Medical Technology, Co., Ltd. Luciferase activity was measured 48 h after miR-30c mimics transfection using a Dual-Luciferase Reporter Assay (Promega Corporation). Data were normalized to *Renilla* luciferase activity.

Cell transfection. For *in vitro* transfection, 100 nM miR-30c-5p mimic (sequence: 5'-UGUAAACAUCCUACACUCUCAGC-3'), miR-30c-5p inhibitor (sequence: 5'-GCUGAGAGUGUAGGAUGUUUACU-3'), miR-30c-5p mimics control (sequence: 5'-CUAACGCAUGCACAGUCGUACG-3') (35), miR-30c-5p inhibitor control (sequence: 5'-CAGUACUUUUGUGUAGUACAA-3') and, which were from Nanjing Synthgene Medical Technology Co., Ltd, were transfected into RPM cells using Lipofectamine 2000 (Invitrogen; Thermo Fisher Scientific, Inc.) for 48 h at 37˚C according to the manufacturer's instructions. miR-30c mimic was co-transfected with 5 μg plasmid pcDNA3.1-SOX9-Flag (Nanjing Synthgene Medical Technology, Co., Ltd.). A total of 5 μg plasmid vector was transferred. For *in vivo* transfection, 5 μg miR-30c mimic, miR-30c inhibitor or controls was transferred into the left ventricle anterior wall of rat myocardium by 8 μl Entranster (Nanjing Synthgene Medical Technology Co., Ltd.). After injection, the chest was closed and the rat was permitted to recover. I/R was performed 48 h later.

Cell viability assay. RPM cells were harvested at 48 h after transfection. Then, 200 μl 0.5 mg/ml MTT solution (Nanjing Synthgene Medical Technology Co., Ltd.) was added to each group and incubated for 4 h at 37˚C. DMSO was used to dissolve purple formazan. Absorbance was detected at a wavelength of 450 nm, as previously described (30).

Statistical analysis. Graphpad Prism 8.0 (GraphPad Software, Inc.) and SPSS 19.0 (IBM Corp.) were used for statistical analysis. Data are presented as the mean ± SD of three independent experiments. Two-tailed unpaired Student's t-test was used to compare two groups. One-way ANOVA followed by

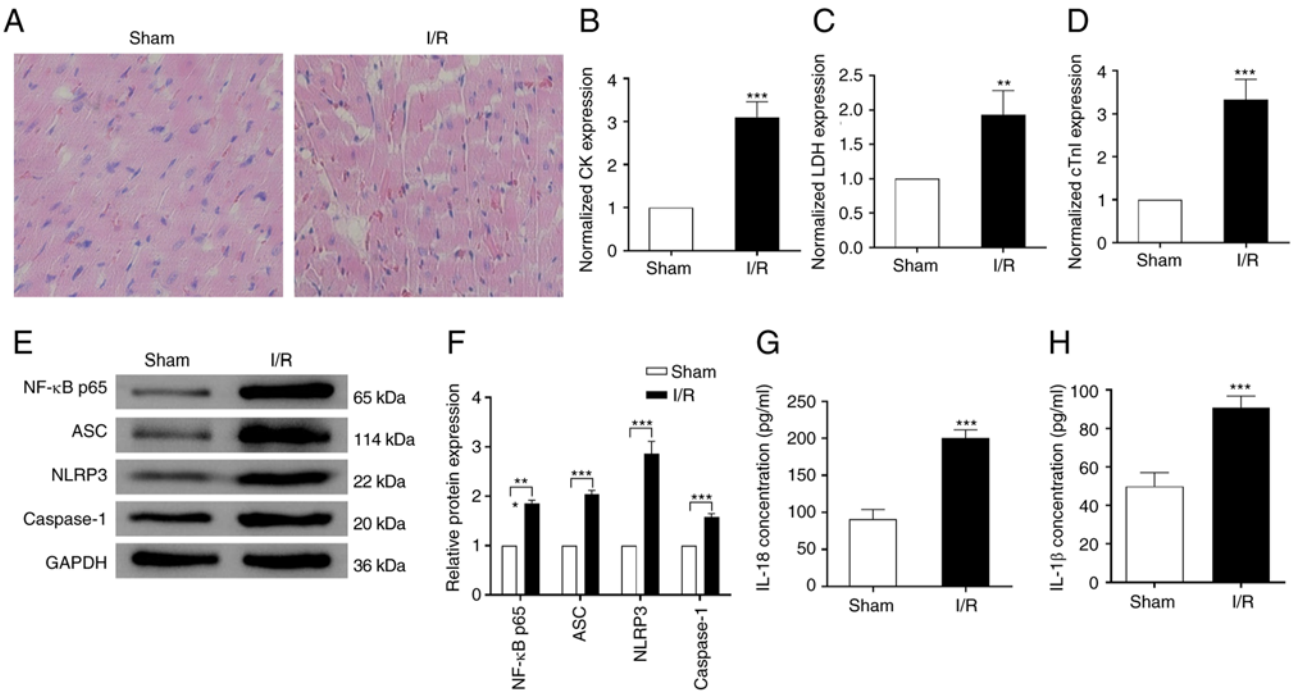

Figure 1. MI/R induces pyroptosis and inflammation *in vivo*. (A) Hematoxylin and eosin staining of rat tissue in Sham and I/R groups (400x). Serum levels of (B) CK, (C) LDH and (D) cTnI were assessed by ELISA following I/R injury. Data are normalized to the Sham group. (E) Protein expression of NF-κB p65, ASC, NLRP3 and caspase-1 was (F) analyzed using western blotting. Serum levels of (G) IL-8 and (H) IL-1β were assessed by ELISA following I/R injury. Data are expressed as the mean ± SD (n=3). *P<0.05, **P<0.01 and ***P<0.001 vs. Sham. MI/R, myocardial ischemia/reperfusion; CK, creatine kinase; LDH, lactate dehydrogenase; cTn, cardiac troponin; ASC, apoptosis-associated speck-like protein containing a caspase recruitment domain.

Tukey's post hoc test was used to compare >2 groups. P<0.05 was considered to indicate a statistically significant difference.

Results

MI/R injury induces pyroptosis and inflammation in vivo. To investigate the effect of MI/R injury on myocardium pyroptosis and inflammation, a rat model of MI/R injury was established. Infiltrating inflammatory cells, myocardial cell swelling, degeneration, cardiac necrosis and loss of transverse striations were observed in the heart subjected to I/R (Fig. 1A). Compared with the sham group, the concentrations of serum CK, LDH, and cTnI were significantly increased in the I/R group (Fig. 1B-D), which suggested successful establishment of the MI/R injury model. Western blotting showed that the expression of pyroptosis-associated protein markers, including ASC, NLRP3 and caspase-1 were significantly upregulated in the rats subjected to I/R injury compared with the sham group. Moreover, the levels of inflammatory marker NF-κB p65 also increased almost 2-fold in the I/R compared with the sham group (Fig. 1E-F). Consistently, following I/R treatment, the expression levels of IL-18 and IL-1β were significantly increased ~2-fold compared with the sham group (Fig. 1G-H). These results indicated that MI/R injury induced myocardium pyroptosis and inflammation *in vivo*.

miR-30c is downregulated and SOX9 is upregulated after I/R treatment in vivo. MI/R induced significant changes in expression of candidate miRNAs, including miR-328a-3p, miR-128-3p, miR-148-3p, miR-676, miR-30d-5p and miR-30c-5p (Fig. 2A-B). Expression levels of miR-328a-3p and miR-128-3p were significantly increased, while expression of miR-30c-5p significantly decreased following MI/R injury (Fig. 2B). In the present study, RNA sequencing showed that fold-change of expression of miR-30c-5p was 1.52 (P=0.0176). The reasons for choosing miR-30c-5p are its high expression following I/R (TagCount, 7,078 vs. 10,736). miRNA-30c-5p has two precursors, MI0000866 and MI0000871, which are slightly different judging from the tags detected in miRNA sequencing. Therefore, two expression data are given. Moreover, the expression levels calculated with the two precursors is almost the same, therefore, the two miRNAs are both miR-30c-5p (Table SI). Expression of SOX9 in rats was detected by western blotting and RT-qPCR. There was significant upregulation of SOX9 expression in the MI/R group at the protein level but no significant change at the mRNA level (Fig. 2C and D).

SOX9 is a target of miR-30c. To confirm the association between miR-30c and SOX9, bioinformatics analysis was performed, which predicted a binding site for miR-30c in the 3'-UTR of WT SOX9 (Fig. 3A). Luciferase activity was significantly reduced by miR-30c transfection in with SOX9 WT, but not MUT UTR (Fig. 3B). Overexpression of miR-30c in RPM cells significantly downregulated the protein expression of SOX9. Conversely, following treatment with miR-30c inhibitor, the protein expression of SOX9 was increased ~2-fold. However, compared with the control, the mRNA expression of SOX9 was not significantly altered following miR-30c mimics or inhibitor transfection (Fig. 3C and D). These data suggested that SOX9 was a direct target of miR-30c.

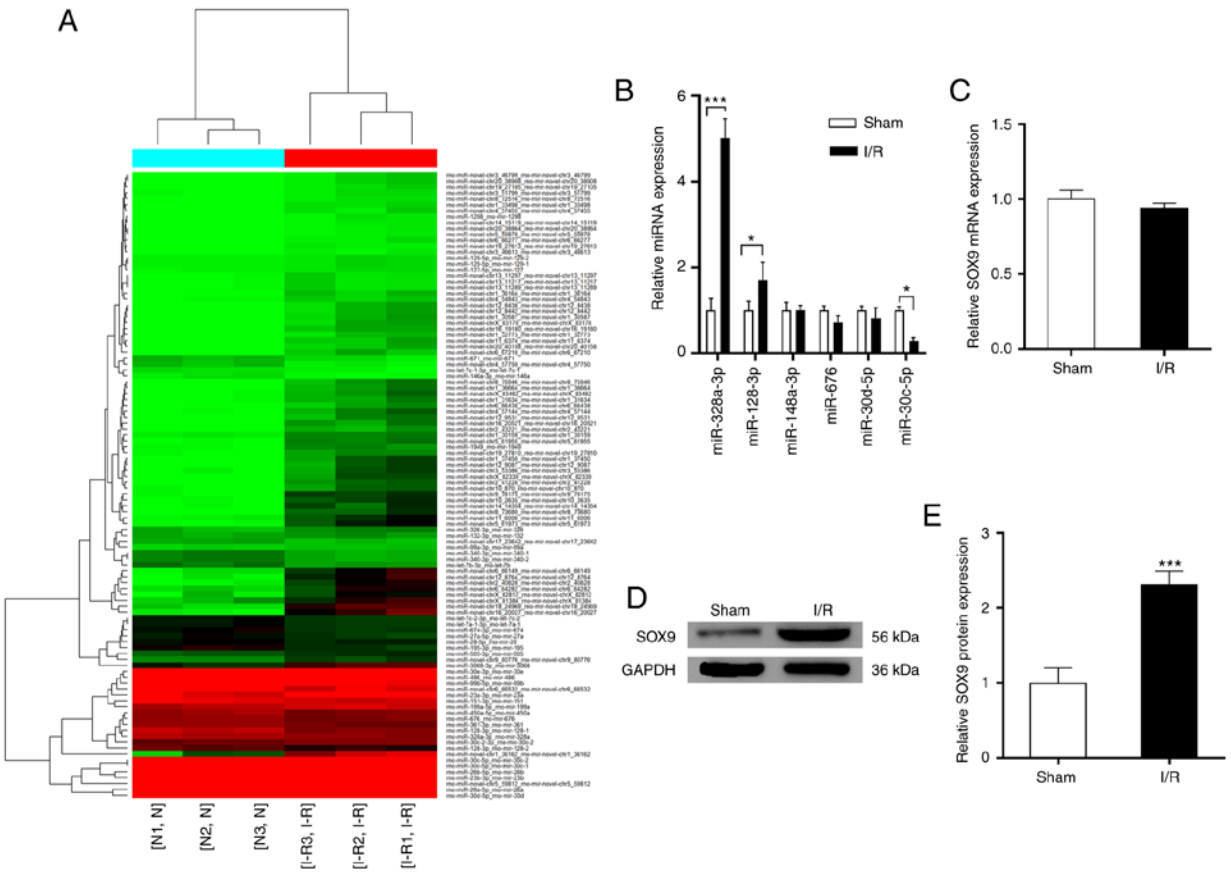

Figure 2. miR-30c expression is downregulated and SOX9 is upregulated in MI/R heart *in vivo*. (A) Expression profile of miRs in sham and I/R model. (B) Expression of miR-328a-3p, miR-128-3p, miR-148-3p, miR-676, miR-30d-5p and miR-30c-5p was measured by RT-qPCR. (C) mRNA level of SOX9 in heart tissue was measured using RT-qPCR. (D) Protein levels of SOX9 in heart tissue were (E) measured using western blotting. Data are expressed as the mean ± SD (n=3). *P<0.05, ***P<0.001 vs. Sham. miR, microRNA; MI/R, myocardial ischemia/reperfusion; RT-q, reverse transcription-quantitative; SOX9, SRY-related high mobility group-box gene 9.

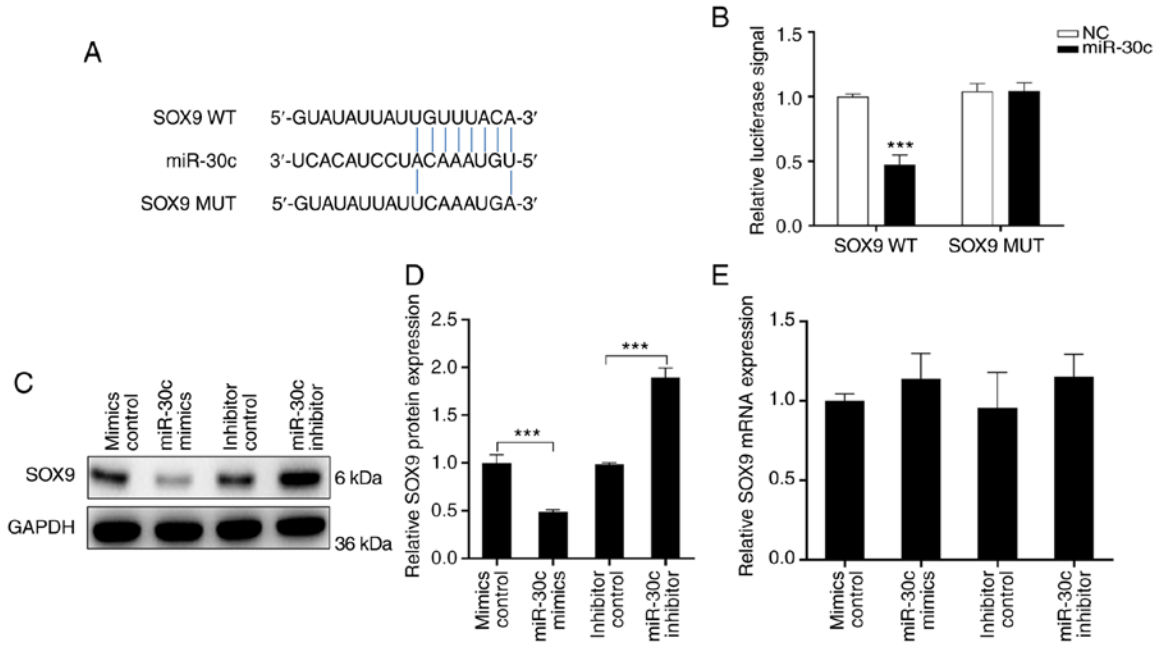

Figure 3. SOX9 is a target gene of miR-30c. (A) Predicted binding sequence for the SOX9 3'UTR with miR-30c. (B) Following transfection with plasmid containing WT SOX9 3'-UTR (pMIR-SOX9-WT) or pMIR-SOX9-MUT, the luciferase activity was measured using dual-luciferase reporter assay. ***P<0.001 vs. NC. (C) SOX9 protein expression was detected by western blotting following miR-30c mimics, miR-30c inhibitor and control transfection and (D) quantified. (E) mRNA expression of SOX9 was assessed by reverse transcription-quantitative PCR following miR-30c mimics, miR-30c inhibitor and control transfection. Data are expressed as the mean ± SD (n=3). ***P<0.001. miR, microRNA; UTR, untranslated region; WT, wild-type; MUT, mutant; SOX9, SRY-related high mobility group-box gene 9; NC, negative control.

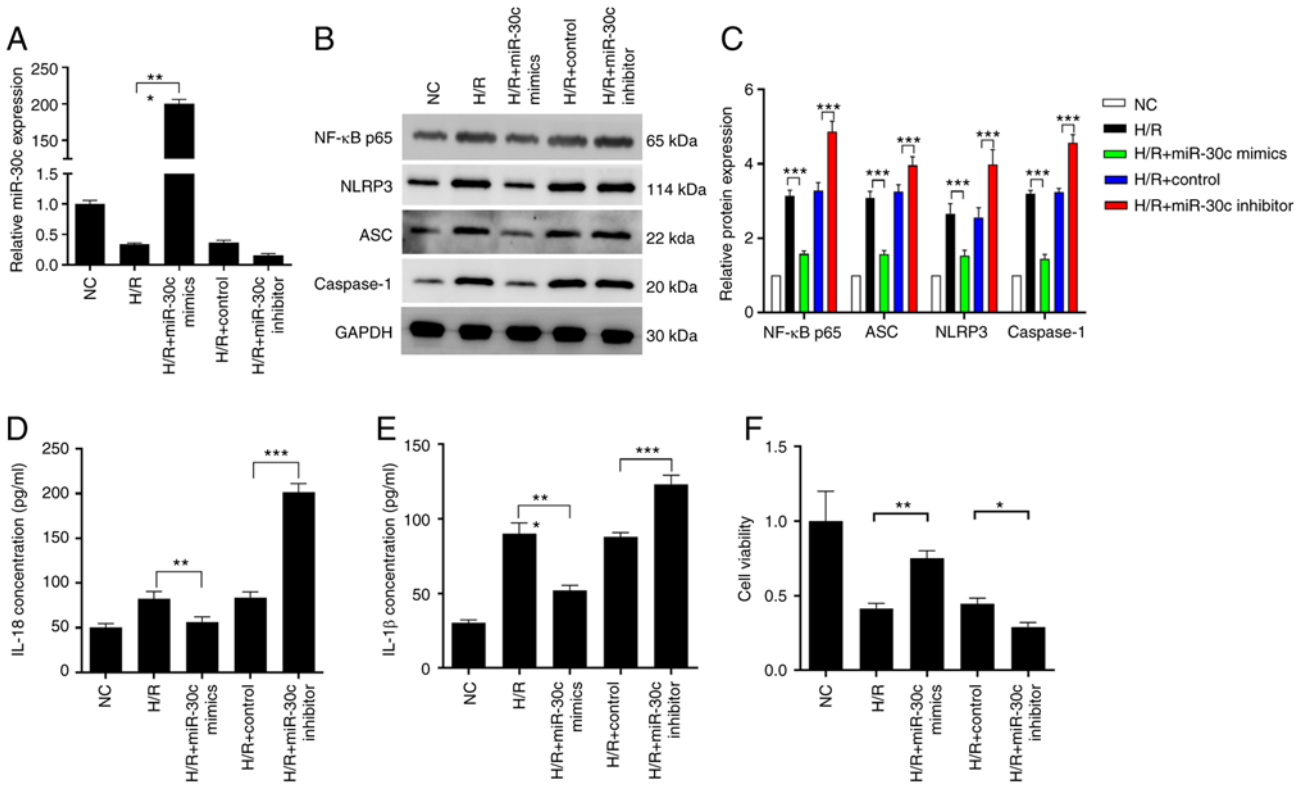

Figure 4. miR-30c inhibits cardiomyocyte pyroptosis under H/R *in vitro*. (A) Expression of miR-30c was assessed by reverse transcription-quantitative PCR following miR-30c mimics, miR-30c inhibitor and control transfection under H/R exposure. (B) Protein expression of (C) NF-κB p65, ASC, NLRP3 and caspase-1 was analyzed by western blotting. Levels of (D) IL-8 and (E) IL-1β were assessed by ELISA after miR-30c mimics, miR-30c inhibitor and control transfection under H/R exposure. (F) Viability of H/R-exposed cells after transfection with miR-30c mimics, miR-30c inhibitor and control. Data are expressed as the mean ± SD (n=3). *P<0.05, **P<0.01, ***P<0.001. NC, negative control; miR, microRNA; H/R, hypoxia/reoxygenation; ASC, apoptosis-associated speck-like protein containing a caspase recruitment domain.

miR-30c inhibits cell pyroptosis in vitro. To investigate the function of miR-30c, H/R exposed cells were transfected with miR-30c mimics or inhibitor. Expression of miR-30c was notably decreased following H/R (Fig. 4A) but increased ~200-fold in RPM cells following transfection with miR-30c mimics. Conversely, expression decreased following transfection with miR-30c inhibitor. After H/R treatment, the protein levels of NF-κB p65, ASC, NLRP3 and caspase-1 in the RPM cells were significantly upregulated. Compared with the H/R group, miR-30c mimics treatment significantly inhibited expression of these proteins. However, inhibition of miR-30c restored the expression of these proteins (Fig. 4B-C). Effects of miR-30c on expression of pro-inflammatory factors IL-18 and IL-1β secreted by RPM cells following H/R exposure was determined using ELISA. Overexpression of miR-30c markedly decreased IL-18 and IL-1β levels in the H/R exposed cells, while these levels were further increased after miR-30c inhibitor transfection (Fig. 4D-E). H/R significantly inhibited primary myocardial cell proliferation. miR-30c mimics treatment reversed the effect of H/R on cell viability (Fig. 4F). Overexpression of miR-30c restored downregulation of SOX9 caused by H/R (Fig. 5A-B). Moreover, overexpression of SOX9 before miR-30c mimics transfection could abolish effects of SOX9. Consistent with these results, the pyroptosis protein markers showed a similar trend (Fig. 5A-D). Expression of IL-1β and IL-18 showed no difference between the H/R + mimics control and H/R + miR-30c mimics + SOX9 overexpression group (Fig. 5B).

SOX9/miR-30c axis regulates MI/R injury in vivo. To confirm the effect of the SOX9/miR-30c axis *in vivo*, MI/R injury rats were treated with miR-30c mimics and miR-30c inhibitor. Compared with the sham group, more infiltrating inflammatory cells, myocardial cell swelling, degeneration, cardiac necrosis and loss of transverse striations were observed in the I/R and I/R + miR-30 inhibitor group. Conversely, it was observed in the present study that the I/R injured heart showed obvious integrity of the myocardial membrane, a normal myofibrillar structure with striations, branched appearance and continuity with adjacent myofibrils after miR-30c mimics treatment (Fig. 6A) (36). According to the results of western blotting, there was notable upregulation in expression of NF-κB p65, ASC, NLRP3, SOX9 and caspase-1 when the rats were subjected to I/R. Elevated expression levels of these proteins were further upregulated by the miR-30c inhibitor transfection. However, the upregulated expression levels of these proteins in the heart of I/R injury rats were restored by miR-30c mimics treatment. (Fig. 6B). Consistently, the levels of cTnI, CK and LDH, key diagnostic markers of MI/R injury (30), were increased in I/R-treated rats compared with the sham group. There was a significant reduction in all these markers following miR-30c mimics transfection. However, following miR-30c inhibitor treatment, the levels of these markers were not significantly decreased (Fig. 6D-F). Similarly, miR-30c mimics decreased serum levels of IL-18 and IL-1β, while miR-30c inhibitor did not significantly affect production of IL-18 and IL-1β (Fig. 6G and H).

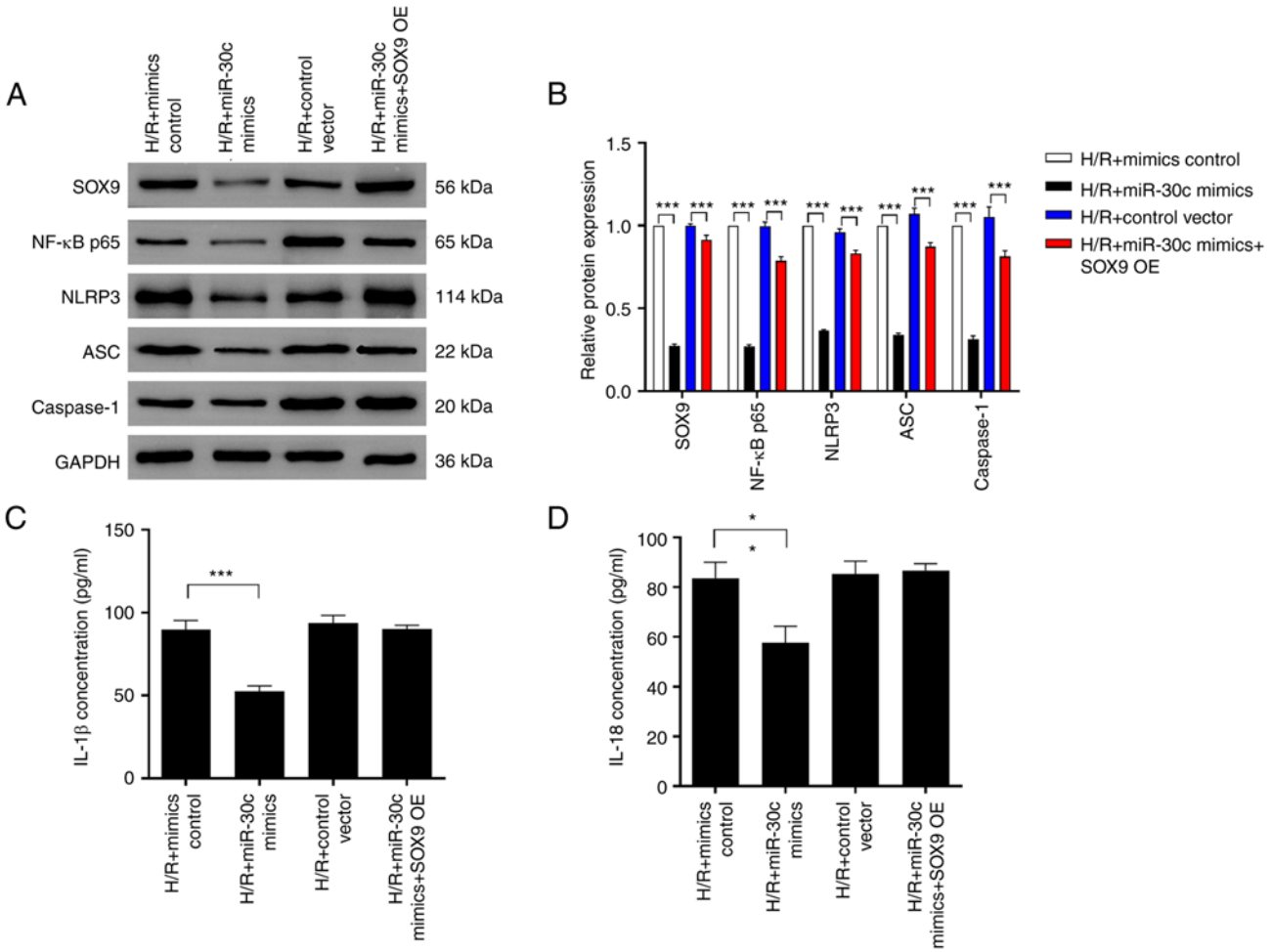

Figure 5. miR-30c decreases pyroptosis via SOX9 *in vitro*. (A) Protein expression levels of NF-κB p65, ASC, NLRP3, caspase-1 and SOX9 were analyzed by western blotting and (B) quantified following miR-30c mimics, miR-30c mimics + SOX9 OE and control transfection. Expression levels of (C) IL-8 and (D) IL-1β were assessed by ELISA following H/R. Data are expressed as the mean ± SD (n=3). *P<0.05 and ***P<0.001. OE, overexpression; miR, microRNA; H/R, hypoxia/reoxygenation; ASC, apoptosis-associated speck-like protein containing a caspase recruitment domain; SOX9, SRY-related high mobility group-box gene 9.

Discussion

The present study aimed to investigate the function and the underlying mechanisms of miRNAs on I/R injury-induced pyroptosis. miR-30c was downregulated, while the expression of SOX9 was upregulated in the MI/R rat model. Overexpression of miR-30c inhibited pyroptosis both *in vivo* and *in vitro*. Furthermore, miR-30c negatively regulated SOX9 expression by binding its 3'UTR.

In the present study, NLRP3 was activated following MI/R injury, which initiates adaptor protein (ASC) cleavage of caspase-1 and IL-1β and IL-18 generation (37). There was a high level of pyroptosis in rats subjected to MI/R or cells treated with H/R. I/R causes cell death, including apoptosis, autophagy, necrosis and pyroptosis. A number of studies have demonstrated that pyroptosis is triggered by NLRP3, AIM2-like receptor proteins and tripartite motif-containing protein and other inflammasomes (38,39). Following the stimulation of these inflammasomes, downstream inflammatory caspase-1 or caspase-11 is cleaved, leading to secretion of pro-inflammatory cytokines IL-1β and IL-18 (40). This process is involved in various types of heart disease, including MI/R injury, myocardial infarction and heart failure (41). For examples, inflammasomes activated by I/R lead to IL-1β production in the heart (42). The accumulation of inflammasomes ASC, cryopyrin and caspase-1 has been observed in an acute myocardial infarction mouse model: Following cryopyrin inhibitor treatment, the formation of inflammasome and infarct size are limited (43). Sandanger *et al* (44) found that compared with WT hearts, a marked improvement of cardiac function and decreased hypoxic damage were present in the hearts of NLRP3-deficient mice subjected to I/R. Therefore, targeting components of pyroptosis may decrease cardiac I/R injury.

miRNAs modulate target genes by binding the 3'UTR of specific mRNAs and may serve a role in the regulation of cardiovascular disease (45). In a rat *in vivo* I/R model, upregulating miR-30c-5p decreases myocardial injury, histopathological changes and apoptosis (46). The reasons for investigating miR-30c-5p are its high expression following I/R and its target gene SOX9 is a transcription factor of the SRY family, which is involved in various cell processes, including oxidation and tumor growth (47). Studies (19, 24) indicate that SOX9 may be involved in the onset of MI/R injury, although the underlying molecular mechanism remains unknown.

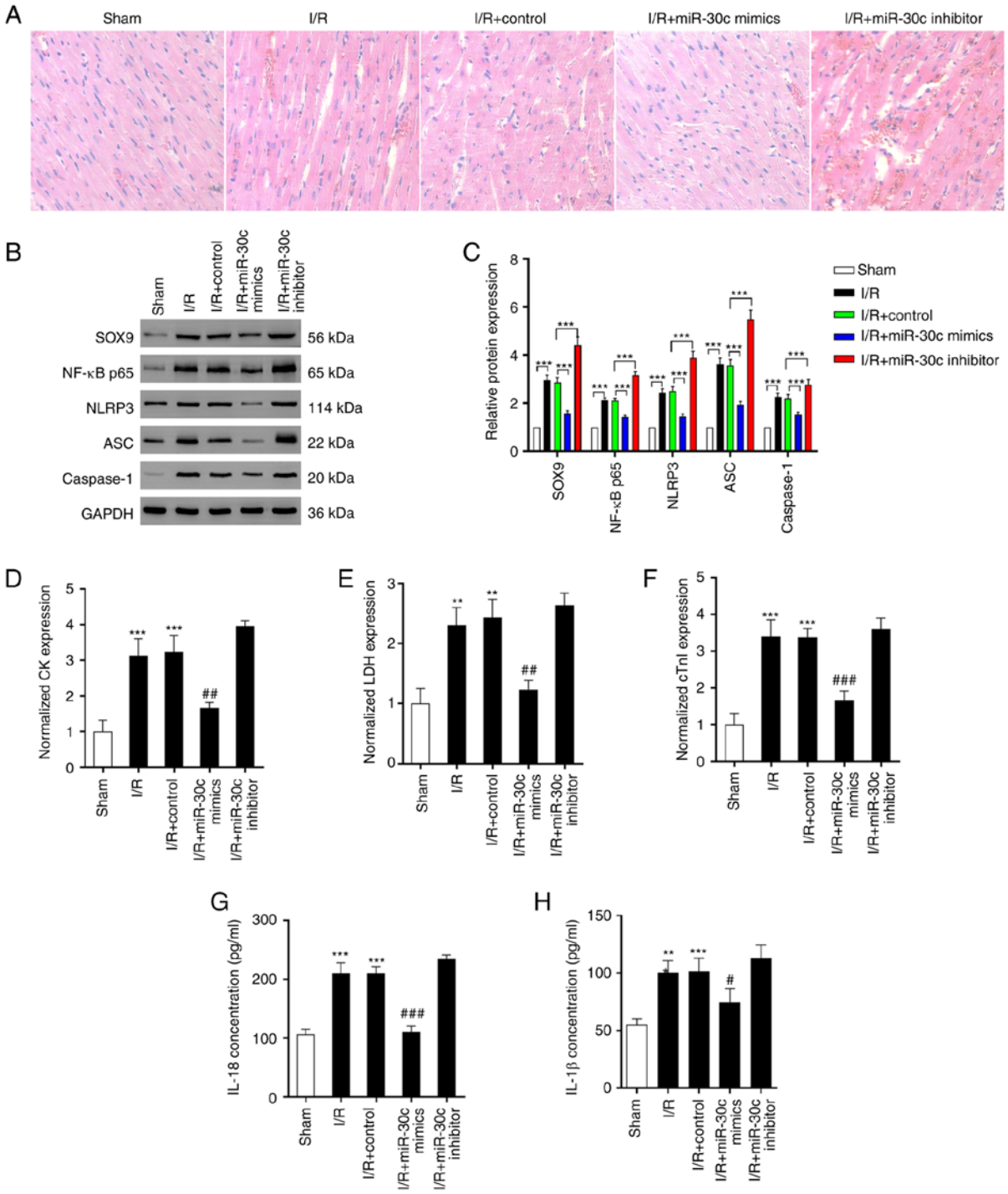

Figure 6. SOX9/miR-30c axis regulates cardiac I/R injury *in vivo*. (A) Hematoxylin and eosin staining of rat tissue (400x magnification). (B) Protein expression of (C) NF-κB p65, ASC, NLRP3, caspase-1 and SOX9 in rat heart tissue. Serum levels of (D) CK, (E) LDH and (F) cTnI were assessed by ELISA. Expression levels of (G) IL-8 and (H) IL-1β were assessed by ELISA. Data are expressed as the mean ± SD (n=3). **P<0.01, ***P<0.001 vs. Sham; $^{\#}$P<0.05, $^{\#\#}$P<0.01, $^{\#\#\#}$P<0.001 vs. I/R + control. CK, creatine kinase; LDH, lactate dehydrogenase; cTn, cardiac troponin; ASC, apoptosis-associated speck-like protein containing a caspase recruitment domain; SOX9, SRY-related high mobility group-box gene 9; I/R, ischemia/reperfusion.

Consistent with the present results, Sun *et al* (48) found that in a rat MI/R model with LAD ligation, miR-30c-5p expression is downregulated. In addition, overexpression of miR-30c inhibits apoptosis, oxidative stress and inflammation both *in vivo* and *in vitro* (48). In addition, overexpression of miR-30c-5p-induced protective effects are associated with its target gene Bach1 and subsequent activation of Nrf2 (48). However, another study found that miR-30c expression is increased in a rat model of MI/R injury and overexpression of miR-30c-5p promotes MI/R injury by activating NF-κB pathway and targeting sirtuin 1 (49). In the aforementioned study (49), LAD was ligated for 30 min before reperfusion for 2 h, while in the present study, following 30 min LAD ligation, hearts were reperfused for 30 min before sample collection. Therefore, both the reperfusion and the sample collection timepoint may be key for miRNA expression

profile. miR-30c-5p can target different signaling pathways during MI/R injury (48,49). The present study reported the association between miR-30c, MI/R injury and pyroptosis. The present study demonstrated that under MI/R injury, SOX9 expression was significantly increased and miR-30c was notably downregulated *in vivo*. miR-30c directly targeted SOX9 by binding the 3'UTR of SOX9. There was no significant difference in mRNA expression of SOX9 however, the protein expression of SOX9 was significantly increased by I/R. It was hypothesized that miR-30c-5p in cardiomyocytes bound to SOX9 mRNA and inhibited SOX9 protein expression but did not directly degrade SOX9 mRNA. This translational suppression mechanism has been discussed by Huntzinger and Izaurralde (50). Overexpression of miR-30c *in vitro* suppressed H/R-induced pyroptosis. Conversely, miR-30c inhibitor treatment promoted the effect of H/R treatment. In addition, overexpression of SOX9 abolished the effect of miR-30c on pyroptosis. Following overexpression of miR-30c *in vivo*, pyroptosis was suppressed and MI/R injury was alleviated. This suggested that regulation of miR-30c expression may contribute to pyroptosis and may serve as a therapeutic target to decrease MI/R injury.

miR-30c decreases the production of reactive oxygen species (ROS) (51,52), which are key for tissue damage and myocardial protection. Furthermore, it is widely reported that overactivation of ROS pathway signaling increases pyroptosis (53,54). During MI/R injury, excessive production ROS and increased pyroptosis of cardiomyocytes may be induced by decreased expression of miR-30c.

In summary, miR-30c was notably downregulated in rats subjected to I/R and directly targeted SOX9. Moreover, miR-30c may serve as a suppressor of cell pyroptosis to decrease I/R-induced heart disease. In the future, gene therapy targeting miR-30c-5p overexpression and SOX9 knockdown may serve a role in MI/R injury clinically.

Acknowledgements

Not applicable.

Funding

The present study was supported by the National Natural Science Foundation of China (grant no. 81860062) and Guizhou Science and Technology Planning Project [grant no. QianKeHeJiChu(2018)1195].

Availability of data and materials

The datasets generated and/or analyzed during the current study are available in the Gene Expression Omnibus repository: ncbi.nlm.nih.gov/geo/query/acc.cgi?acc=GSE221780.

Authors' contributions

JN, WZ, SY and SC performed the experiments, wrote the manuscript and constructed figures. HW and TY conceived and designed the experiments and provided reagents. JN and HW confirm the authenticity of all the raw data. All authors have read and approved the final manuscript.

Ethics approval and consent to participate

Animal experiments were approved [approval no. KLLY(A)-2019-008] by Zunyi Medical University Committee (Guizhou, China).

Patient consent for publication

Not applicable.

Competing interests

The authors declare that they have no competing interests.

References

1. Hausenloy DJ and Yellon DM: Ischaemic conditioning and reperfusion injury. Nat Rev Cardiol 13: 193-209, 2016.
2. Ibanez B, Heusch G, Ovize M and Van de Werf F: Evolving therapies for myocardial ischemia/reperfusion injury. J Am Coll Cardiol 65: 1454-1471, 2015.
3. Eltzschig HK and Eckle T: Ischemia and reperfusion-from mechanism to translation. Nat Med 17: 1391-1401, 2011.
4. Han J, Wang D, Ye L, Li P, Hao W, Chen X, Ma J, Wang B, Shang J, Li D and Zheng Q: Rosmarinic acid protects against inflammation and cardiomyocyte apoptosis during myocardial ischemia/reperfusion injury by activating peroxisome proliferator-activated receptor gamma. Front Pharmacol 8: 456, 2017.
5. Makkos A, Ágg B, Petrovich B, Varga ZV, Görbe A and Ferdinandy P: Systematic review and network analysis of microRNAs involved in cardioprotection against myocardial ischemia/reperfusion injury and infarction: Involvement of redox signalling. Free Radic Biol Med 172: 237-251, 2021.
6. Jayawardena E, Medzikovic L, Ruffenach G and Eghbali M: Role of miRNA-1 and miRNA-21 in acute myocardial ischemia-reperfusion injury and their potential as therapeutic strategy. Int J Mol Sci 23: 1512, 2022.
7. Marinescu MC, Lazar AL, Marta MM, Cozma A and Catana CS: Non-coding RNAs: Prevention, diagnosis, and treatment in myocardial ischemia-reperfusion injury. Int J Mol Sci 23: 2728, 2022.
8. Lorenzen JM, Batkai S and Thum T: Regulation of cardiac and renal ischemia-reperfusion injury by microRNAs. Free Radic Biol Med 64: 78-84, 2013.
9. Hinkel R, Penzkofer D, Zuhlke S, Fischer A, Husada W, Xu QF, Baloch E, van Rooij E, Zeiher AM, Kupatt C and Dimmeler S: Inhibition of microRNA-92a protects against ischemia/reperfusion injury in a large-animal model. Circulation 128: 1066-1075, 2013.
10. Hullinger TG, Montgomery RL, Seto AG, Dickinson BA, Semus HM, Lynch JM, Dalby CM, Robinson K, Stack C, Latimer PA, *et al*: Inhibition of miR-15 protects against cardiac ischemic injury. Circ Res 110: 71-81, 2012.
11. Wang JX, Zhang XJ, Li Q, Wang K, Wang Y, Jiao JQ, Feng C, Teng S, Zhou LY, Gong Y, *et al*: MicroRNA-103/107 regulate programmed necrosis and myocardial ischemia/reperfusion injury through targeting FADD. Circ Res 117: 352-363, 2015.
12. Wang X, Zhang X, Ren XP, Chen J, Liu H, Yang J, Medvedovic M, Hu Z and Fan GC: MicroRNA-494 targeting both proapoptotic and antiapoptotic proteins protects against ischemia/reperfusion-induced cardiac injury. Circulation 122: 1308-1318, 2010.
13. He Y, Cai Y, Sun T, Zhang L, Irwin MG, Xu A and Xia Z: MicroRNA-503 exacerbates myocardial ischemia/reperfusion injury via inhibiting PI3K/Akt- and STAT3-Dependent prosurvival signaling pathways. Oxid Med Cell Longev 2022: 3449739, 2022.
14. Lee TL, Lai TC, Lin SR, Lin SW, Chen YC, Pu CM, Lee IT, Tsai JS, Lee CW and Chen YL: Conditioned medium from adipose-derived stem cells attenuates ischemia/reperfusion-induced cardiac injury through the microRNA-221/222/PUMA/ETS-1 pathway. Theranostics 11: 3131-3149, 2021.
15. Song R, Dasgupta C, Mulder C and Zhang L: MicroRNA-210 controls mitochondrial metabolism and protects heart function in myocardial infarction. Circulation 145: 1140-1153, 2022.

16. Shah S, Esdaille CJ, Bhattacharjee M, Kan HM and Laurencin CT: The synthetic artificial stem cell (SASC): Shifting the paradigm of cell therapy in regenerative engineering. Proc Natl Acad Sci USA 119, 2022.
17. Kubo Y, Beckmann R, Fragoulis A, Conrads C, Pavanram P, Nebelung S, Wolf M, Wruck CJ, Jahr H and Pufe T: Nrf2/ARE signaling directly regulates SOX9 to potentially alter age-dependent cartilage degeneration. Antioxidants (Basel) 11: 263, 2022.
18. Gong X, Li Y, He Y and Zhou F: USP7-SOX9-miR-96-5p-NLRP3 network regulates myocardial injury and cardiomyocyte pyroptosis in sepsis. Hum Gene Ther 33: 1073-1090, 2022.
19. Rui L, Liu R, Jiang H and Liu K: Sox9 Promotes cardiomyocyte apoptosis after acute myocardial infarction by promoting miR-223-3p and inhibiting MEF2C. Mol Biotechnol 64: 902-913, 2022.
20. Fan XD, Zheng HB, Fan XS and Lu S: Increase of SOX9 promotes hepatic ischemia/reperfusion (IR) injury by activating TGF-β1. Biochem Biophys Res Commun 503: 215-221, 2018.
21. Yang B, Nie Y, Wang L and Xiong W: Flurbiprofen axetil protects against cerebral ischemia/reperfusion injury via regulating miR-30c-5p and SOX9. Chem Biol Drug Des 99: 197-205, 2022.
22. Scharf GM, Kilian K, Cordero J, Wang Y, Grund A, Hofmann M, Froese N, Wang X, Kispert A, Kist R, *et al*: Inactivation of Sox9 in fibroblasts reduces cardiac fibrosis and inflammation. JCI Insight 5: e126721, 2019.
23. Schauer A, Adams V, Poitz DM, Barthel P, Joachim D, Friedrich J, Linke A and Augstein A: Loss of Sox9 in cardiomyocytes delays the onset of cardiac hypertrophy and fibrosis. Int J Cardiol 282: 68-75, 2019.
24. Lacraz GPA, Junker JP, Gladka MM, Molenaar B, Scholman KT, Vigil-Garcia M, Versteeg D, de Ruiter H, Vermunt MW, Creyghton MP, *et al*: Tomo-Seq Identifies SOX9 as a key regulator of cardiac fibrosis during ischemic injury. Circulation 136: 1396-1409, 2017.
25. Cheng N, Li L, Wu Y, Wang M, Yang M, Wei S and Wang R: microRNA-30e up-regulation alleviates myocardial ischemia-reperfusion injury and promotes ventricular remodeling via SOX9 repression. Mol Immunol 130: 96-103, 2021.
26. Li J, Wei Y, Zhou J, Zou H, Ma L, Liu C, Xiao Z, Liu X, Tan X, Yu T and Cao S: Activation of locus coeruleus-spinal cord noradrenergic neurons alleviates neuropathic pain in mice via reducing neuroinflammation from astrocytes and microglia in spinal dorsal horn. J Neuroinflammation 19: 123, 2022.
27. Health NIo: Guide for the care and use of laboratory animals. National Academies, 1985.
28. Douglas KL, Piccirillo CA and Tabrizian M: Cell line-dependent internalization pathways and intracellular trafficking determine transfection efficiency of nanoparticle vectors. Eur J Pharm Biopharm 68: 676-687, 2008.
29. Wang K, Liu CY, Zhou LY, Wang JX, Wang M, Zhao B, Zhao WK, Xu SJ, Fan LH, Zhang XJ, *et al*: APF lncRNA regulates autophagy and myocardial infarction by targeting miR-188-3p. Nat Commun 6: 6779, 2015.
30. Cao S, Liu Y, Sun W, Zhao L, Zhang L, Liu X and Yu T: Genome-Wide expression profiling of anoxia/reoxygenation in rat cardiomyocytes uncovers the role of MitoKATP in energy homeostasis. Oxid Med Cell Longev 2015: 756576, 2015.
31. Liu W, Huang L, Liu X, Zhu L, Gu Y, Tian W, Zhang L, Deng S and Yu T: Urocortin I protects against myocardial ischemia/reperfusion injury by sustaining respiratory function and cardiolipin content via mitochondrial ATP-Sensitive potassium channel opening. Oxid Med Cell Longev 2022: 7929784, 2022.
32. Wang QL, Li TT, Fang CL and Zhang BL: Bioinformatics analysis of the wheel treadmill test on motor function recovery after spinal cord injury. Ibrain 7: 265-277, 2021.
33. Cao S, Zhang D, Yuan J, Liu C, Zhou W, Zhang L, Yu S, Qin B, Li Y and Deng W: MicroRNA And circular RNA expression in affected skin of patients with postherpetic neuralgia. J Pain Res 12: 2905-2913, 2019.
34. Deng W, Wang Y, Long X, Zhao R, Wang Z, Liu Z, Cao S and Shi B: miR-21 Reduces Hydrogen Peroxide-Induced Apoptosis in c-kit^{+} Cardiac stem cells in vitro through PTEN/PI3K/Akt signaling. Oxid Med Cell Longev 2016: 5389181, 2016.
35. Cui L, Yu M and Cui X: MiR-30c-5p/ROCK2 axis regulates cell proliferation, apoptosis and EMT via the PI3K/AKT signaling pathway in HG-induced HK-2 cells. Open Life Sci 15: 959-970, 2020.
36. Chang X, Zhang K, Zhou R, Luo F, Zhu L, Gao J, He H, Wei T, Yan T and Ma C: Cardioprotective effects of salidroside on myocardial ischemia-reperfusion injury in coronary artery occlusion-induced rats and Langendorff-perfused rat hearts. Int J Cardiol 215: 532-544, 2016.
37. Yajima N, Takahashi M, Morimoto H, Shiba Y, Takahashi Y, Masumoto J, Ise H, Sagara J, Nakayama J, Taniguchi S and Ikeda U: Critical role of bone marrow apoptosis-associated speck-like protein, an inflammasome adaptor molecule, in neointimal formation after vascular injury in mice. Circulation 117: 3079-3087, 2008.
38. Xiao L, Magupalli VG and Wu H: Cryo-EM structures of the active NLRP3 inflammasome disc. Nature 613: 595-600, 2023.
39. McKee CM and Coll RC: NLRP3 inflammasome priming: A riddle wrapped in a mystery inside an enigma. J Leukoc Biol 108: 937-952, 2020.
40. Jorgensen I, Rayamajhi M and Miao EA: Programmed cell death as a defence against infection. Nat Rev Immunol 17: 151-164, 2017.
41. Yu Y, Shi H, Yu Y, Liu M, Li M, Liu X, Wang Y and Chen R: Inhibition of calpain alleviates coxsackievirus B3-induced myocarditis through suppressing the canonical NLRP3 inflammasome/caspase-1-mediated and noncanonical caspase-11-mediated pyroptosis pathways. Am J Transl Res 12: 1954-1964, 2020.
42. Kawaguchi M, Takahashi M, Hata T, Kashima Y, Usui F, Morimoto H, Izawa A, Takahashi Y, Masumoto J, Koyama J, *et al*: Inflammasome activation of cardiac fibroblasts is essential for myocardial ischemia/reperfusion injury. Circulation 123: 594-604, 2011.
43. Mezzaroma E, Toldo S, Farkas D, Seropian IM, Van Tassell BW, Salloum FN, Kannan HR, Menna AC, Voelkel NF and Abbate A: The inflammasome promotes adverse cardiac remodeling following acute myocardial infarction in the mouse. Proc Natl Acad Sci USA 108: 19725-19730, 2011.
44. Sandanger O, Ranheim T, Vinge LE, Bliksøen M, Alfsnes K, Finsen AV, Dahl CP, Askevold ET, Florholmen G, Christensen G, *et al*: The NLRP3 inflammasome is up-regulated in cardiac fibroblasts and mediates myocardial ischaemia-reperfusion injury. Cardiovasc Res 99: 164-174, 2013.
45. Dong XJ, Chen JJ, Xue LL and Al-hawwas M: Treadmill training improves cognitive function by increasing IGF2 targeted down-regulation of miRNA-483. Ibrain 8: 264-275, 2022.
46. Meng S, Hu Y, Zhu J, Feng T and Quan X: miR-30c-5p acts as a therapeutic target for ameliorating myocardial ischemia-reperfusion injury. Am J Transl Res 13: 2198-2212, 2021.
47. Luanpitpong S, Li J, Manke A, Brundage K, Ellis E, McLaughlin SL, Angsutararux P, Chanthra N, Voronkova M, Chen YC, *et al*: SLUG is required for SOX9 stabilization and functions to promote cancer stem cells and metastasis in human lung carcinoma. Oncogene 35: 2824-2833, 2016.
48. Sun M, Guo M, Ma G, Zhang N, Pan F, Fan X and Wang R: MicroRNA-30c-5p protects against myocardial ischemia/reperfusion injury via regulation of Bach1/Nrf2. Toxicol Appl Pharmacol 426: 115637, 2021.
49. Chen J, Zhang M, Zhang S, Wu J and Xue S: Rno-microRNA-30c-5p promotes myocardial ischemia reperfusion injury in rats through activating NF-κB pathway and targeting SIRT1. BMC Cardiovasc Disord 20: 240, 2020.
50. Huntzinger E and Izaurralde E: Gene silencing by microRNAs: Contributions of translational repression and mRNA decay. Nat Rev Genet 12: 99-110, 2011.
51. Jung YD, Park SK, Kang D, Hwang S, Kang MH, Hong SW, Moon JH, Shin JS, Jin DH, You D, *et al*: Epigenetic regulation of miR-29a/miR-30c/DNMT3A axis controls SOD2 and mitochondrial oxidative stress in human mesenchymal stem cells. Redox Biol 37: 101716, 2020.
52. Wang X, Zhang Y, Han S, Chen H, Chen C, Ji L and Gao B: Overexpression of miR-30c-5p reduces cellular cytotoxicity and inhibits the formation of kidney stones through ATG5. Int J Mol Med 45: 375-384, 2020.
53. Zheng D, Liu J, Piao H, Zhu Z, Wei R and Liu K: ROS-triggered endothelial cell death mechanisms: Focus on pyroptosis, parthanatos, and ferroptosis. Front Immunol 13: 1039241, 2022.
54. Abais JM, Xia M, Zhang Y, Boini KM and Li PL: Redox regulation of NLRP3 inflammasomes: ROS as trigger or effector? Antioxid Redox Signal 22: 1111-1129, 2015.